Bacteriophage Lambda gpNu1 and *Escherichia coli* IHF Proteins Cooperatively Bind and Bend Viral DNA: Implications for the Assembly of a Genome-Packaging Motor†

Marcos E. Ortega¶ and Carlos E. Catalano*,‡,§

Department of Pharmaceutical Sciences, Department of Biochemistry and Molecular Genetics, and the Molecular Biology Program, University of Colorado Health Sciences Center, Denver, Colorado 80262

Received November 7, 2005; Revised Manuscript Received February 1, 2006

ABSTRACT: Terminase enzymes are common to both prokaryotic and eukaryotic double-stranded DNA viruses and are responsible for packaging viral DNA into the confines of an empty procapsid shell. In all known cases, the holoenzymes are heteroligomers composed of a large subunit that possesses the catalytic activities required for genome packaging and a small subunit that is responsible for specific recognition of viral DNA. In bacteriophage lambda, the DNA recognition protein is gpNu1. The gpNu1 subunit interacts with multiple recognition elements within *cos*, the packaging initiation site in viral DNA, to site-specifically assemble the packaging machinery. Motor assembly is modulated by the *Escherichia coli* integration host factor protein (IHF), which binds to a consensus sequence also located within *cos*. On the basis of a variety of biochemical data and the recently solved NMR structure of the DNA binding domain of gpNu1, we proposed a novel DNA binding mode that predicts significant bending of duplex DNA by gpNu1 (de Beer et al. (2002) *Mol. Cell 9*, 981−991). We further proposed that gpNu1 and IHF cooperatively bind and bend viral DNA to regulate the assembly of the packaging motor. Here, we characterize cooperative gpNu1 and IHF binding to the *cos* site in lambda DNA using a quantitative electrophoretic mobility shift (EMS) assay. These studies provide direct experimental support for the long presumed cooperative assembly of gpNu1 and IHF at the *cos* sequence of lambda DNA. Further, circular permutation experiments demonstrate that the viral and host proteins each introduce a strong bend in *cos*-containing DNA, but not nonspecific DNA substrates. Thus, specific recognition of viral DNA by the packaging apparatus is mediated by both DNA sequence information and by structural alteration of the duplex. The relevance of these results with respect to the assembly of a viral DNA-packaging motor is discussed.

Terminase enzymes are common to many double-stranded DNA (dsDNA)[1] viruses of both prokaryotic and eukaryotic origin (*1*−*3*). These enzymes are responsible for DNA packaging, the ATP-dependent insertion of viral DNA into an empty, preformed procapsid. In most cases, the preferred packaging substrate is a linear concatemer of multiple genomes linked in a head-to-tail fashion (immature DNA) (*2*−*5*). Terminase enzymes excise an individual genome from the concatemer and concomitantly translocate the "matured" DNA into the procapsid. All of the characterized terminase enzymes share common structural and functional characteristics; they are heteroligomers composed of a large subunit, which provides the packaging activities of the enzyme, and a small subunit that is responsible for specific recognition of viral DNA (*2*−*4*, *6*). In the case of bacteriophage lambda terminase, the larger gpA subunit (73.3 kDa) possesses all the catalytic activities required to mature and package viral DNA. This includes nuclease, helicase, ATPase, and DNA translocase catalytic activities (*7*−*13*). The smaller gpNu1 subunit (20.4 kDa) is responsible for specific assembly of the packaging machinery at *cos*, the packaging initiation site in the lambda genome (*13*−*16*).

The *cos* sequence demarcates the junction between individual genomes in the concatemer and is the site where terminase assembles to initiate the packaging process (*4*, *13*). The gpA subunit cuts the duplex at the *cosN* subsite to mature the DNA (Figure 1A) (*8*, *11*, *16*). Specific assembly of the packaging motor is mediated by gpNu1, which binds to three R-elements within the *cosB* subsite (*17*, *18*). The *Escherichia coli* integration host factor stimulates virus yield in vivo (*19*−*21*) and DNA maturation in vitro (*8*, *11*, *22*−*25*). An integration host factor protein (IHF) consensus binding sequence is also located within *cosB*, and it has been

† This work was supported by National Institutes of Health Grant GM063943.

* Address correspondence to this author at University of Colorado School of Pharmacy, 4200 E. Ninth Ave, C238, Denver, CO 80262. Phone, (303) 315-8561; fax, (303) 315-6281 (fax); e-mail, carlos.catalano@uchsc.edu.

‡ Department of Pharmaceutical Sciences.

§ Molecular Biology Program.

¶ Department of Biochemistry and Molecular Genetics.

[1] Abbreviations: β-ME, 2-mercaptoethanol; ***cos***, cohesive end site of the lambda genome; *cos*-DNA, a 272 bp duplex that contains the entire lambda *cos* sequence; *cosB*, the subsite where gpNu1 binds to assembly the packaging motor; *cosB*-DNA, a 135 bp duplex that contains the only *cosB* sequence of the lambda genome; *cos2*-DNA, a 94 bp duplex that contains the R3-I1-R2 sequence of the lambda genome; *cosN*, the subsite where the terminase gpA subunit introduces symmetric nicks 12 bases apart in the duplex to mature concatemeric DNA; dsDNA, double-stranded DNA; EMS, electromobility shift; ns-DNA, a 272 bp duplex of random sequence; wHTH, winged helix-turn-helix DNA binding motif.

10.1021/bi052284b CCC: $33.50
Published on Web 04/04/2006

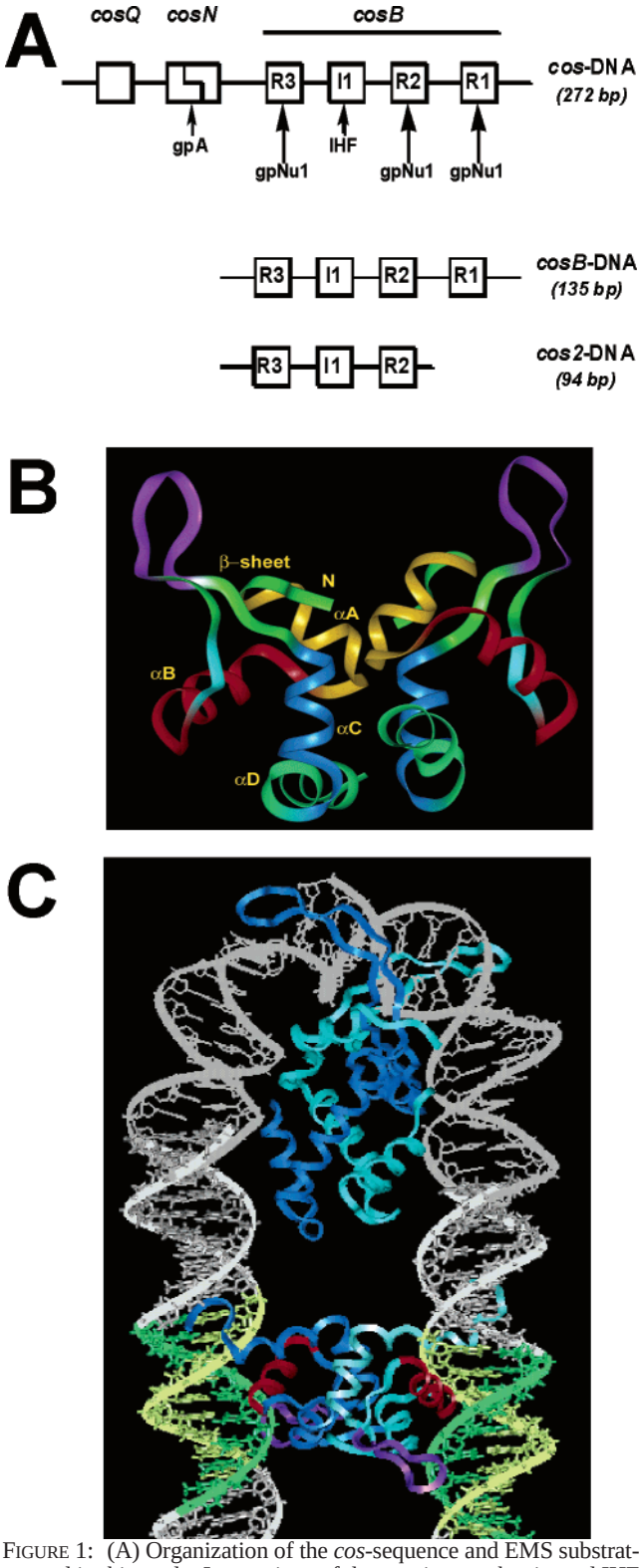

FIGURE 1: (A) Organization of the *cos*-sequence and EMS substrates used in this study. Interactions of the terminase subunits and IHF with elements within the *cos* sequence are indicated at top. (B) Ribbon representation of the gpNu1 DNA binding domain, taken with permission from de Beer et al. (*32*). Copyright 2002 Elsevier, Inc. The wing residues and the HTH recognition helix (αB helix) are colored purple and red, respectively. (C) Model for cooperative binding and bending of *cos*-DNA by gpNu1 and IHF, taken with permission from de Beer et al. (*32*). Copyright 2002 Elsevier, Inc. The IHF dimer is displayed in a ribbon representation with each subunit colored a different shade of blue. The R2 and R3 elements are displayed in green. The gpNu1 DBD is displayed with the HTH motifs and wing residues colored as in panel B, while the remainder of the two monomers is shown in different shades of blue for simplicity.

proposed, but never demonstrated, that gpNu1 and IHF act in concert to assemble the packaging motor. An understanding of how these proteins interact with viral DNA to initiate genome packaging is central to a molecular description of virus assembly.

Structural and biochemical characterization of gpNu1 has been frustrated by aggregation of the isolated subunit at elevated concentrations (*14*, *26*−*28*). Mutagenesis studies have revealed that a hydrophobic region of the protein extending between residues 100 and 140 is responsible for aggregation of the protein, and this hydrophobic region is referred to as the "self-association domain" of gpNu1 (*27*). Biochemical, biophysical, and structural studies have demonstrated that deletion of the self-association domain affords highly soluble protein dimers in the concentration range of 5 μM to 2 mM (*29*, *30*). These studies have further shown that the N-terminal 55 residues of gpNu1 represent a structural and functional DNA-binding domain of the protein (*29*−*33*). The high-resolution solution structure of the gpNu1ΔE68 dimer, a deletion construct consisting of the N-terminal 68 residues of gpNu1, was recently solved in our lab (*32*) and is shown in Figure 1B. This structure has yielded insight into how gpNu1 recognizes *cos* to initiate DNA packaging. Specifically, the gpNu1ΔE68 dimer possesses a pair of winged helix-turn-helix (wHTH) DNA binding motifs that lie on opposite faces of the dimer and point away from each other; this geometry precludes binding of the DBD dimer to two adjacent half-sites, a DNA binding mode common to dimeric HTH-containing DNA-binding proteins such as the lambda repressor (*34*). On the basis of the structure of the gpNu1ΔE68 dimer, a variety of biochemical data and the sequence organization of *cosB*, we proposed a novel DNA-binding mode for gpNu1, as shown in Figure 1C. In this model, the wHTH motifs in each subunit of the dimer bind to R-element half-sites separated by 40 base pairs in the duplex. This requires that a significant bend be introduced into *cos*-DNA upon gpNu1 binding. Consistent with this hypothesis, an IHF consensus-binding element is observed exactly midway between the R3 and R2 elements of *cosB* (Figure 1A). In all characterized cases, IHF binds to its cognate binding element and introduces a strong bend in the duplex, which provides a structure conducive to the assembly of additional proteins on the modified duplex structure (*35*−*38*). Thus, we proposed that gpNu1 and IHF cooperatively bind and bend *cos*-DNA to assemble the packaging motor.

Here, we report the results of experiments that directly test the gpNu1 DNA-binding and bending model previously proposed. We demonstrate that full-length gpNu1 and IHF bind in a cooperative manner to *cos*-containing DNA, but not to nonspecific DNA substrates. We further demonstrate that gpNu1 binding to *cos*-DNA introduces a strong bend in the duplex, similar to that introduced by IHF. The implications of these results with respect to the assembly of a viral DNA-packaging motor are discussed.

EXPERIMENTAL PROCEDURES

Materials and Methods. Tryptone, yeast extract, and agar were purchased from DIFCO. Restriction endonuclease enzymes, the Klenow fragment, and T4 polynucleotide kinase were purchased from Invitrogen. DEAE-sepharose FF, SP-sepharose FF, and Q-sepharose FF chromatography resins

were purchased from Pharmacia. Radionucleotides were purchased from Amersham. Bio-6 spin columns were purchased from Bio-Rad. The pBend2 vector was purchased from the American Type Culture Collection. All of the synthetic oligonucleotides used in these studies were purchased from Invitrogen and were used without further purification. All other materials were of the highest quality commercially available.

Bacterial cultures were grown in shaker flasks utilizing a New Brunswick Scientific series 25 incubator-shaker. All protein purifications utilized a Pharmacia FPLC system, which consisted of two P500 pumps, a GP250-plus controller, a V7 injector, and a Uvicord SII variable wavelength detector. UV−vis absorbance spectra were recorded on a Hewlett-Packard HP8452A spectrophotometer. Automated DNA sequence analysis was performed by the University of Colorado Cancer Center Macromolecular Resources Core facility.

Protein Purification. GpNu1-C114A was used in all of the studies reported here. This mutant protein possesses wild-type DNA binding, ATPase, and *cos*-cleavage endonuclease activities, but is more stable during prolonged storage (Ortega and Catalano, manuscript in preparation). GpNu1-C114A was expressed in BL21(DE3) [pC114A] cells and purified from inclusion bodies as described by Hanagan et al. (*39*); herein, we refer to the mutant protein as gpNu1 for simplicity. *E. coli* IHF was purified from HN880 (a kind gift of Howard Nash, National Institutes of Health, Bethesda, MD) by the method of Nash et al. (*40*). The purified proteins were homogeneous as determined by SDS−PAGE and densitometer analysis as previously described (*23*).

Preparation of the DNA Substrates Used in the Electrophoretic Mobility Shift (EMS) Studies. DNA fragments used in the EMS experiments were prepared by large-scale preparative PCR using pAFP1 as a template. This plasmid, a generous gift of Dr. Michael Feiss (University of Iowa), contains the entire *cos* sequence cloned into a pUC19 background. The plasmid was purified from *E. coli* JM107 [pAFP1] cells using Qiagen DNA prep columns according to the manufacturer's protocol. PCR primers were designed to amplify (i) the entire *cos* sequence (*cos*-DNA), (ii) only the *cosB* sequence (*cosB*-DNA), (iii) the sequence encompassing the *R2*, *I1*, and *R3* elements (*cos2*-DNA), and (iv) a 272 base pair duplex of random sequence (ns-DNA) (see Figure 1A). All of the PCR primers contained *Nde*1 restriction endonuclease sites at their 5′ ends to be used for subsequent radiolabeling of the purified PCR products. The PCR reaction mixtures (200 μL per tube) contained 250 μmol of each primer, 10 ng of pAFP1 template, and PCR supermix (Invitrogen) as recommended by the manufacturer; the total reaction volumes were 1−3 mL. PCR cycles were as follows: (94 °C for 1 min, 50 °C for 1 min, 72 °C for 2 min) × 50 cycles. The pooled PCR reaction mixtures were loaded onto a 1 mL Q-Sepharose column by gravity flow. The column was washed with TE (pH 8) containing 630 mM NaCl to remove unincorporated primers, and the amplified PCR products were then eluted with TE containing 800 mM NaCl. The eluted fragments were precipitated with EtOH and resuspended in TE (pH 8) for storage. The purity of each DNA product was verified by 1% agarose gel analysis, and the concentration of DNA was determined by UV−vis spectroscopy (*41*).

Each DNA substrate was digested with *Nde*1 restriction endonuclease, and the major fragments were isolated on a 0.8% agarose gel and purified using the Qiagen gel extraction kit. The substrates were then 3′-end-labeled at both ends using α^{32}P-dATP and the Klenow fragment according to the manufacturer's recommended protocol.

Electrophoretic Mobility Shift Experiments. Equilibrium binding experiments were performed in buffer containing 20 mM Tris, pH 8, 1 mM EDTA, 2 mM spermidine, 50 mM NaCl, 7 mM β-ME, and 10% glycerol. Radiolabeled DNA was included at a concentration of 1−10 pM, and herring sperm DNA (100 pM) was added to all binding mixtures. IHF and/or gpNu1 was added as indicated in each individual experiment, and the binding mixture was incubated at room temperature for 15 min. Unless otherwise indicated, the mixture was then loaded onto an 8% polyacrylamide gel (acrylamide/bis-acrylamide ratio of 80:1), and the gels were run at 15 V/cm in 0.5× TBE at 4 °C for 1.5 h. The gel was then dried in vacuo on Whatman 3MM filter paper, and the radioactive bands were visualized and quantified using a Molecular Dynamics Storm system and the Molecular Dynamics ImageQuant data analysis package. The fraction of bound DNA was calculated using

$$\text{Fraction Bound} = \frac{(\text{counts in retarded band})}{(\text{counts in retarded band} + \text{counds in free DNA band})} \quad (1)$$

Analysis of the EMS Data. The raw binding data were analyzed according to

$$\text{Fraction Bound} = b + (m - b)\left[\frac{K^n[\text{P}]^n}{(1 + K^n[\text{P}]^n)}\right] \quad (2)$$

where [P] is the protein concentration, K is the apparent equilibrium association constant ($K_{A,app}$), n is the Hill coefficient, b is the baseline offset, and m is the fraction of DNA bound at saturation (*42*). Note that this equation reduces to a simple Langmuir binding equation if n is held constant at 1. The experimental data were fit using the Igor data analysis program (Wave Metrics, Lake Oswego, OR).

Preparation of the DNA Substrates Used in the Circular Permutation Studies. The DNA substrates used in the permutation experiments were prepared as described by Kim et al. (*43*) using the minimal *cos2*-DNA sequence as the target bending sequence. Briefly, *cos2*-DNA (Figure 1A) was amplified by PCR as described above, except that the primers contained *Xba*1 restriction sites at their 5′ ends rather than *Nde*1 sites. The PCR reaction mixture was extracted with phenol/chloroform, and the amplified DNA was precipitated with EtOH. The fragment was taken into TE (pH 8), digested with *Xba*1, and again isolated as described above. The DNA was then resuspended in TE (pH 8) and cloned into *Xba*-digested pBend2. This plasmid is a derivative of pBR322 that contains 17 unique restriction sites as direct repeats flanking a central *Xba*1 cloning site (see Figure 5A) (*43*). The resulting plasmid (pBendCos2) was transfected into *E. coli* DH5α cells, and colonies were screened for the presence of the insert by restriction analysis.

Preparative purification of pBendCos2 was performed using Qiagen DNA prep columns. A family of five bending

substrates was generated by digestion of the plasmid with *Mlu*1, *Nhe*1, *EcoR*V, *Nru*1, and *BamH*1 restriction endonucleases, respectively, as shown in Figure 5A. Each of the five fragments (214 bp) was isolated from a 0.8% agarose gel and purified using the Qiagen gel extraction kit. Gel purity was verified by 1% agarose gel analysis, and the fragments were 5′-radiolabeled using γ^{32}P-ATP and T4 polynucleotide kinase as recommended by the supplier.

Circular Permutation Experiments. The binding reaction conditions were as described above for the EMS experiments, except that the DNA bending fragment (*Mlu*1, *Nhe*1, *EcoR*V, *Nru*1, or *BamH*1, Figure 5A) was included at 250 counts per μL (100−500 pM; identical results were obtained for each DNA substrate within this concentration range, not shown). IHF and gpNu1 were included as indicated in each individual experiment. The protein·DNA complexes were fractionated on an 8% polyacrylamide gel (acrylamide/bisacrylamide ratio of 80:1), and the radioactive bands were quantified as described above. Analysis of DNA bending was by the method of Thompson and Landy (*44*) using the following equation:

$$\frac{\mu_M}{\mu_E} = \frac{\cos \alpha}{2} \quad (3)$$

where μ_M is the migration of the complex with the bend located centrally in the DNA duplex, μ_E is the migration of the complex with the bend at the end of the DNA duplex, and α is the bend angle.

RESULTS

IHF and gpNu1 Binding to cos-DNA and Nonspecific DNA Substrates. Initial EMS studies were performed with *cos*-DNA, a 272 base pair fragment that encompasses the entire *cos*-sequence (Figure 1A) and ns-DNA, a nonspecific DNA fragment of identical size but that has no sequence homology to the *cos* sequence. We first examined IHF binding to *cos*-DNA. As anticipated, a single retarded complex is observed (Figure 2A,B, inset) consistent with the single IHF consensus binding sequence in *cos*-DNA (see Figure 1A). IHF also binds to ns-DNA and with an affinity that is only 4-fold less than that observed with the *cos*-DNA substrate (see Table 1). That IHF discriminates only modestly between specific and nonspecific DNA substrates has been reported previously (*45*). In contrast to *cos*-DNA, however, IHF binds to the ns-DNA substrate weakly and without the formation of a discrete band in the gel (Figure 2A).

We next examined gpNu1 binding to *cos*-DNA, which yielded unexpected results as follows. First, gpNu1 binds to *cos*-DNA to yield a single retarded band at all subsaturating concentrations of the protein (Figure 2A,C, inset). This is surprising because gpNu1 specifically interacts with all three of the R-elements in *cosB*, and we thus expected to see three distinct complexes in the titration profile. This phenomenon is discussed in more detail below. Second, gpNu1 also binds to ns-DNA, similarly yielding a single gel-retarded band; however, the nonspecific DNA complex migrates at a position quite distinct from that formed with *cos*-DNA (Figure 2A). Third, the affinity of gpNu1 for *cos*-containing DNA is only ≈2-fold greater than that of ns-DNA (Figure 2C, Table 1). The data suggest that, while gpNu1 discriminates only modestly between *cos*-DNA and ns-DNA substrates, the nucleoprotein complex formed at the *cos* sequence differs in a fundamental way from that formed at a random DNA sequence.

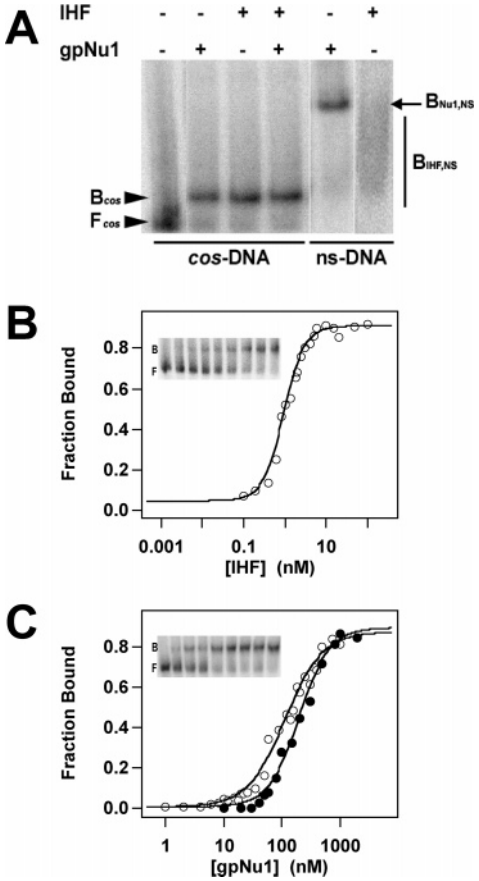

FIGURE 2: IHF and gpNu1 bind to *cos*-DNA and ns-DNA substrates. (A) Autoradiogram of an EMS experiment with gpNu1 and IHF binding to *cos*-DNA. The incubation mixtures contained either *cos*-DNA or ns-DNA substrates as indicated below the autoradiogram. IHF (10 nM) and/or gpNu1 (300 nM) was included as indicated at the top of the figure and the EMS experiment performed as described in Experimental Procedures, except that a 5% gel was used in this experiment. The positions of unbound *cos*-DNA (F_{cos}) and the specific nucleoprotein complexes formed with IHF and gpNu1 (B_{cos}) are indicated with arrowheads. The unbound ns-DNA substrate migrates at a position identical to that of *cos*-DNA (not shown). The position of the nonspecific gpNu1 nucleoprotein complex is indicated with an arrow ($B_{Nu1,NS}$). IHF binds to ns-DNA to form a weak complex that migrates as a smear on the gel ($B_{IHF,NS}$). (B) IHF was incrementally added to *cos*-DNA as indicated (○). Each data point represents the average of at least three independent experiments (standard deviation 3%−5%, omitted for clarity), and the solid lines represent the best fit of the data to eq 2 as described in Experimental Procedures. The inset shows an autoradiogram of a typical titration experiment with the IHF concentration increasing from left to right. F and B indicate the positions of free and bound DNA, respectively. Note that a single retarded complex is observed at all protein concentrations. (C) Increasing concentrations of gpNu1 were added to *cos*-DNA (○) or to ns-DNA (●) as indicated. Each data point represents the average of at least three independent experiments (standard deviation 3%−5%, omitted for clarity), and the solid line represents the best fits of the data to eq 2 as described in Experimental Procedures. The inset shows an autoradiogram of a typical titration experiment with the gpNu1 concentration increasing from left to right. F and B indicate the positions of free and bound DNA, respectively. Note that a single retarded complex is observed at all protein concentrations.

Table 1: Analysis of Protein Binding to *cos*-DNA and ns-DNA Substrates[a]

	cos-DNA		ns-DNA	
protein	$K_{D,app}$	*n*	$K_{D,app}$	*n*
gpNu1	118 ± 9 nM	1.32 ± 0.12	201 ± 16 nM	1.50 ± 0.18
IHF	1.00 ± 0.07 nM	1.74 ± 0.19	*b*	*b*

[a] The data presented in Figure 2 were quantified as described in Experimental Procedures. [b] IHF binds to ns-DNA to yield a complex that migrates as a "smear" on the gel (see Figure 2A). Therefore, the affinity of IHF for ns-DNA was not rigorously defined, but it is roughly 4-fold lower than for *cos*-DNA.

Finally, we were quite surprised by the observation that the gpNu1·*cos*-DNA complex migrates at a position identical to that obtained with IHF. Moreover, the ternary gpNu1·IHF·*cos*-DNA complex migrates at a position identical to those of the binary protein·DNA complexes (Figure 2A). This result is particularly surprising given the differences in size (40.8 vs 20.5 kDa) and charge (pI = 4.97 and 9.37) of gpNu1 and IHF, respectively (*14*, *46*). We attempted to resolve the gpNu1 and IHF nucleoprotein complexes by altering the EMS buffer conditions (pH, salt, etc.), by altering the gel composition (higher/lower polyacrylamide concentration and/or cross-linking, polyacrylamide−agarose gels), and by using larger format gels; however, these attempts were uniformly unsuccessful (data not shown).

GpNu1 and IHF Bind Cooperatively to cos-DNA. IHF plays an important role in lambda development. In vivo and in vitro data suggest that the host protein is involved in assembly of the packaging motor at *cos*, and cooperative assembly of gpNu1 and IHF at *cosB* has been proposed, but never demonstrated (*11*, *21*−*24*, *47*). We therefore utilized the EMS assay to directly probe for cooperative binding of the two proteins. We note that each protein binds to *cos*-DNA to yield a single complex and that the mobility of the complexes are identical. Moreover, a single complex with identical mobility is observed in the presence of saturating concentrations of both proteins (see Figure 2A). This complicates a quantitative analysis of cooperative binding using EMS methods. Nevertheless, Figure 3A,B clearly demonstrates that the affinity of gpNu1 for *cos*-DNA is significantly increased in the presence of subsaturating concentrations of IHF. Similarly, the affinity of IHF for *cos*-DNA is strongly affected by subsaturating concentrations of gpNu1 (Figure 3C,D). In contrast, neither protein affects the binding of the other to nonspecific DNA substrates (not shown). Thus, the data clearly demonstrate specific and cooperative binding interactions between gpNu1 and IHF at the lambda *cos* sequence.

GpNu1 Binds to Minimal cos Substrates. We previously proposed that gpNu1 binding to *cosB* introduces a strong bend in the duplex similar to that imposed by IHF (*32*). To directly test this hypothesis, we needed to define a minimal DNA substrate suitable for use in the circular permutation experiments described below. Therefore, the EMS experiment was performed as described in Experimental Procedures except that *cosB*-DNA or *cos2*-DNA fragments (Figure 1A) were used as binding substrates. As shown in Figure 4A, both of these fragments yield a single, specific complex with

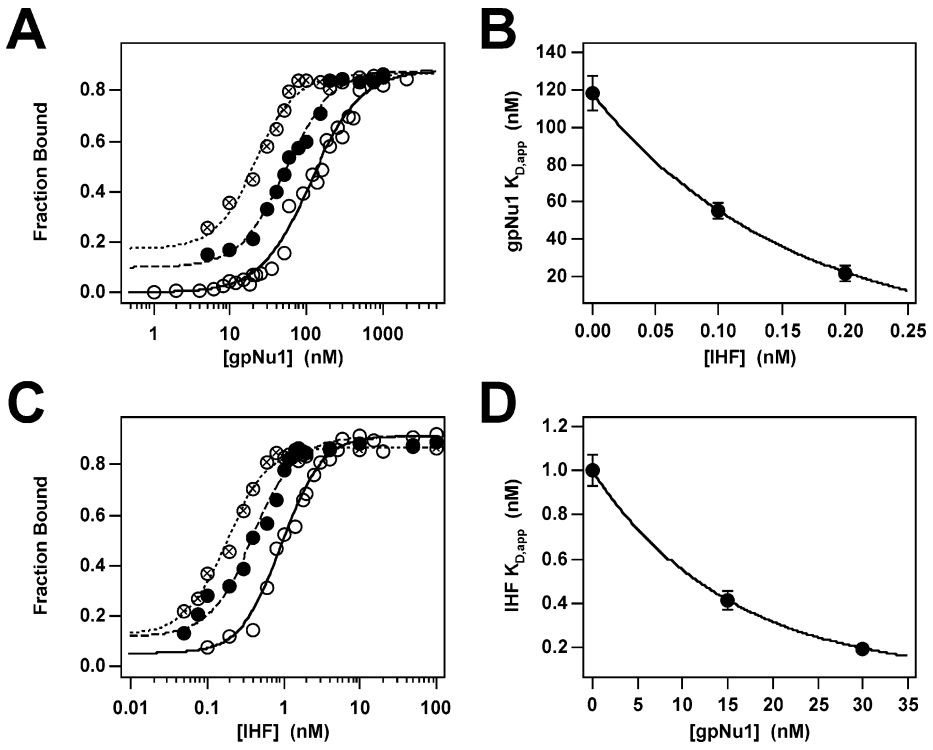

FIGURE 3: Cooperative binding of gpNu1 and IHF at *cos*. (A) Increasing concentrations of gpNu1 were added to *cos*-DNA in the absence (○) or presence of 0.1 nM (●) or 0.2 nM (⊗) IHF, as indicated. Each data point represents the average of at least three separate experiments (standard deviation 3%−5%, omitted for clarity), and the solid lines represent the best fit of the data as described in Experimental Procedures. (B) The data in panel A were analyzed as described in Experimental Procedures, and the $K_{D,app}$ for gpNu1 is plotted as a function of [IHF]. These data are summarized in Table 2. (C) Increasing concentrations of IHF were added to *cos*-DNA in the absence (○) or presence of 15 nM (●) or 30 nM (⊗) gpNu1, as indicated. Each data point represents the average of at least three separate experiments (standard deviation 5%−9%, omitted for clarity), and the solid lines represent the best fit of the data as described in Experimental Procedures. (D) The data in panel C were analyzed as described in Experimental Procedures, and the $K_{D,app}$ for IHF is plotted as a function of [gpNu1]. These data are summarized in Table 2.

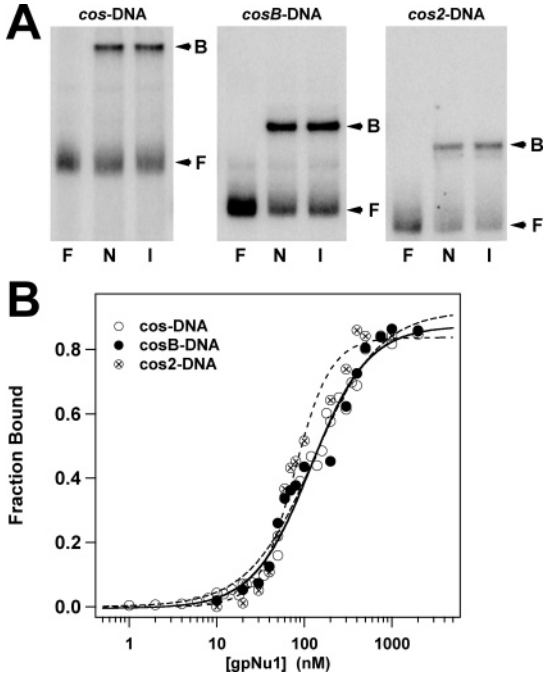

FIGURE 4: GpNu1 binds to minimal *cos*-DNA substrates. (A) Left, center, and right panels show autoradiograms of EMS studies with *cos*-DNA (272 bp), *cosB*-DNA (135 bp), and *cos2*-DNA (94 bp), respectively (see Figure 1A). In each panel, F is free DNA (no protein), N is DNA plus 100 nM gpNu1, and I is DNA plus 0.5 nM IHF. (B) Increasing concentrations of gpNu1 were added to *cos*-DNA (○), *cosB*-DNA (●), or *cos2*-DNA (⊗), as indicated. Each data point represents the average of at least three separate experiments (standard deviation 3%−5%, omitted for clarity), and the solid lines represent the best-fit curves to the data as described in Experimental Procedures. These data are summarized in Table 3.

Table 2: Cooperative Binding of GpNu1 and IHF to *cos*-DNA[a]

titrated Protein	additions	$K_{D,app}$	*n*
gpNu1	none	118 ± 9 nM	1.32 ± 0.12
gpNu1	0.1 nM IHF	55 ± 4 nM	1.46 ± 0.17
gpNu1	0.2 nM IHF	22 ± 2 nM	1.66 ± 0.22
IHF	none	1.00 ± 0.07 nM	1.74 ± 0.19
IHF	15 nM gpNu1	0.41 ± 0.04 nM	1.55 ± 0.20
IHF	30 nM gpNu1	0.19 ± 0.01 nM	1.59 ± 0.15

[a] The data presented in Figure 3A,C were quantified as described in Experimental Procedures.

Table 3: GpNu1 Binds to Minimal *cos*-DNA Substrates[a]

protein	DNA substrate	$K_{D,app}$	*n*
gpNu1	*cos*-DNA	118 ± 9 nM	1.32 ± 0.12
gpNu1	*cosB*-DNA	129 ± 25 nM	1.16 ± 0.17
gpNu1	*cos2*-DNA	77 ± 5 nM	2.11 ± 0.28

[a] The data presented in Figure 4B were quantified as described in Experimental Procedures.

gpNu1. Moreover, similar to the full *cos*-DNA sequence, the minimal substrates yield a single IHF·DNA complex that migrates identically to those obtained with gpNu1. Again, all attempts to resolve these complexes by alteration of the EMS conditions were unsuccessful. Of note, the affinity of gpNu1 for the minimal *cos*-duplexes is essentially identical to that observed with the entire *cos* sequence (Figure 4B, Table 3). This indicates that the minimal *cos2*-DNA substrate retains all of the determinants necessary for binding by gpNu1 and is therefore suitable for use in the DNA bending experiments described below.

GpNu1 and IHF Bend cos2-DNA. To test the hypothesis that gpNu1 introduces bending into *cos*-DNA, we used a circular permutation assay to probe for alteration in duplex structure. The minimal *cos2* sequence described above was used as a target sequence as outlined in Figure 5A. We first examined IHF-induced bending as a positive control. Figure 5B shows that IHF binding to *cos2*-DNA yields the characteristic "frown" in the circular permutation experiment, indicating DNA bending by the protein. Analysis of the data indicates that IHF introduces a 120 ± 5° bend in *cos*-DNA, a value slightly less than that previously reported[2] (*36*, *43*, *44*). We next examined gpNu1 binding to *cos2*-DNA, and the data are presented in Figure 5C. The figure clearly shows that gpNu1 yields a gel migration pattern identical to that obtained with IHF. Moreover, the observed "frown" is essentially identical in the presence of saturating concentrations of both proteins (data not shown). Analysis of the data according to eq 3 indicates that gpNu1 binding to *cos2*-DNA introduces a 133 ± 3° bend in the duplex, while the duplex in the ternary gpNu1·IHF·*cos2*-DNA complex is bent by 137 ± 4°.

DISCUSSION

Terminase enzymes are a central component of the genome-packaging motors in both prokaryotic and eukaryotic dsDNA viruses. The small terminase subunits are responsible for specific recognition of viral DNA and site-specific assembly of the packaging machinery. GpNu1 is the small terminase subunit of bacteriophage lambda, and specific recognition of viral DNA is mediated by interactions of gpNu1 with the R-elements of *cosB*. The goal of this work is to define the protein·DNA interactions responsible for specific assembly of the DNA packaging motor at *cos*.

Early models for motor assembly proposed that gpNu1 dimers bind cooperatively to the three R-elements of *cosB*, a mechanism analogous to lambda repressor binding to the O_R/O_L operators of the lambda genome (*48*, *49*). This model predicts that three distinct protein·DNA complexes should be observed in a gpNu1 titration experiment with *cos*-DNA. Thus, it was initially surprising that a single gpNu1·*cos*-DNA complex is observed at all intermediate protein concentrations in the EMS experiments. Even more perplexing was the observation that the gpNu1·*cos*-DNA complex comigrates with the IHF·*cos*-DNA complex despite the distinct physical properties of the two proteins. Importantly, this migration pattern is a sequence-specific effect as gpNu1 and IHF each bind nonspecific DNA substrates to yield complexes of distinct mobility.

A physical interpretation of the EMS data remained elusive until the high-resolution structure of the gpNu1 DNA-binding domain (gpNu1-DBD) was solved in our lab (*32*). The structure reveals that the gpNu1-DBD forms a dimer with C2 symmetry in which the wHTH DNA-binding motifs face

[2] Published values for IHF-induced bending range from 140° in solution (Kosturko, et al. (1989) *Nucleic Acids Res. 17*, 317−333) to 160° in the crystal structure (Rice et al. (1996) *Cell 87*, 1295−1306). The apparent extent of protein-induced DNA bending in solution is underestimated as the length of the DNA increases due to dynamic bending of the duplex (Landy, A. (1989) *Annu. Rev. Biochem. 58*, 913−949). DNA duplexes of 25 and 120 bp were used in the crystallographic and solution studies, respectively, while our studies used a 214 bp binding substrate (see Figure 5A). Thus, the slightly smaller bend angle measured here likely reflects additional duplex flexibility in the IHF·*cos*-DNA complex.

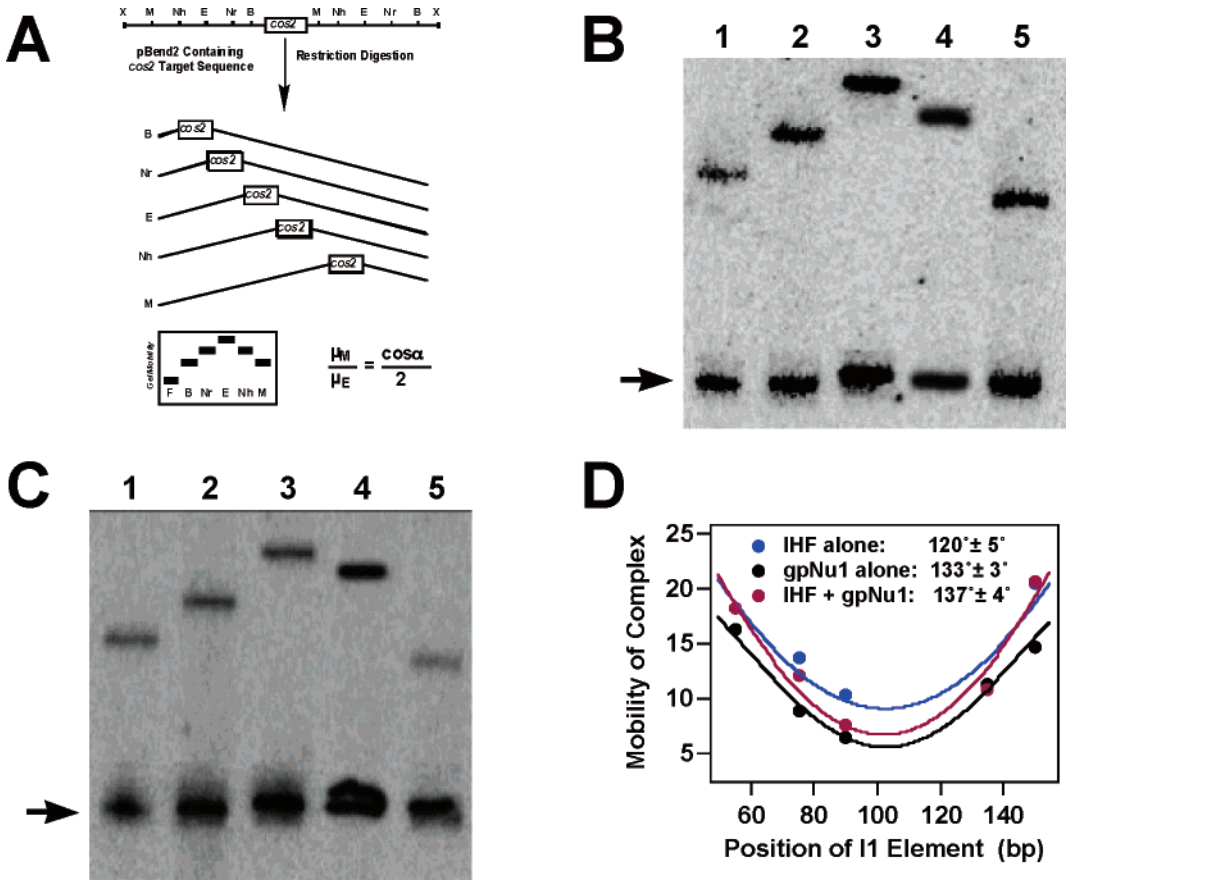

FIGURE 5: IHF and gpNu1 bend *cos*-DNA. (A) The circular permutation assay. Restriction digestion of pBendCos2 with *Mlu*1, *Nhe*1, *EcoR*V, *Nru*1, and *BamH*1 affords five products of equal length (214 bp) but with the *cos2* sequence located at differing positions along the duplex. Bending of the duplex at the *cos2* sequence will result in altered mobility of the various fragments yielding a diagnostic "frown" pattern, shown in a cartoon representation. (B) Autoradiogram of a circular permutation experiment with IHF. Lanes 1−5 are the *BamH*1, *Nru*1, *EcoR*V, *Nhe*1, and *Mlu*1 fragments, respectively, in the presence of 0.5 nM IHF. (C) Autoradiogram of a circular permutation experiment with gpNu1. Lanes 1−5 are the *BamH*1, *Nru*1, *EcoR*V, *Nhe*1, and *Mlu*1 fragments, respectively, in the presence of 100 nM gpNu1. The position of free DNA is indicated with an arrow. (D) Plot of the relative mobility of bound complexes versus position of *I1* element in DNA sequence. Each data point represents the average of at least three separate experiments.

away from each other (see Figure 1B). This geometry precludes a conventional DNA-binding mode where the HTH motifs bind to half-sites in a palindromic recognition sequence as is observed in a variety of repressor protein systems (*34*, *50*, *51*). Thus, the historical model for gpNu1 binding to *cosB* (cooperative assembly of three dimers) is seriously challenged by the biochemical and structural data. In light of this, we proposed a novel model for gpNu1 recognition of *cosB*, where an isolated protein dimer simultaneously binds two R-element "half-sites" that are spatially separated in the duplex (*32*). The hypothesis is supported by model-building studies and predicts that gpNu1 binding to *cosB* should introduce a strong bend in the duplex (Figure 1C).

The data presented here clearly establish that gpNu1 indeed introduces a strong bend in *cos*-DNA and that the R3-I1-R2 elements are sufficient for specific and high-affinity binding. Interestingly, the bend introduced by gpNu1 is similar to that introduced by IHF, a well-characterized DNA bending protein. This suggests that the two proteins form similar nucleoprotein complexes as predicted by the binding and bending model. Further, the data provide a mechanistic explanation for cooperative assembly of gpNu1 and IHF at *cos*, as shown in Figure 6A. Binding of the first protein must overcome the energetic penalty required to bend the duplex. Binding of the second partner is now more favorable as the energetic cost of duplex bending has been "paid for" by the first protein. In other words, binding of either protein to a pre-bent duplex is energetically favorable. Within this context, we note that the I1 element of *cosB* introduces an intrinsic bend into the duplex (20−30°; (*52*))[3] and that mutation of bases that reduce the intrinsic bend render the virus strongly dependent on IHF (*21*). We presume that this results from the inability of gpNu1 alone to bend the duplex and a failure to assemble the packaging machinery at *cos*.

As outlined above, the EMS experiments yielded two surprising observations. The first was that the gpNu1·*cos*-DNA complex (a 40.8 kDa acidic protein) comigrates with that formed with IHF (a 20.5 kDa basic protein). The binding and bending model proposed in Figure 1C is consistent with this observation, as follows. We suggest that the mobility of the gpNu1 and IHF nucleoprotein complexes is dominated by the architecture of the DNA, that is, a bent duplex. Importantly, the ternary gpNu1·IHF·*cos*-DNA complex migrates at an identical position as the binary complexes, again suggesting that the dominant factor is DNA structure. In contrast, nucleoprotein complexes formed with nonspecific DNA substrates migrate quite distinctly, suggesting that duplex bending is dependent on sequence-specific interactions, as proposed.

[3] The presence of an intrinsic bend in unbound *cos*-DNA is evident in the circular permutation studies shown in Figure 5.

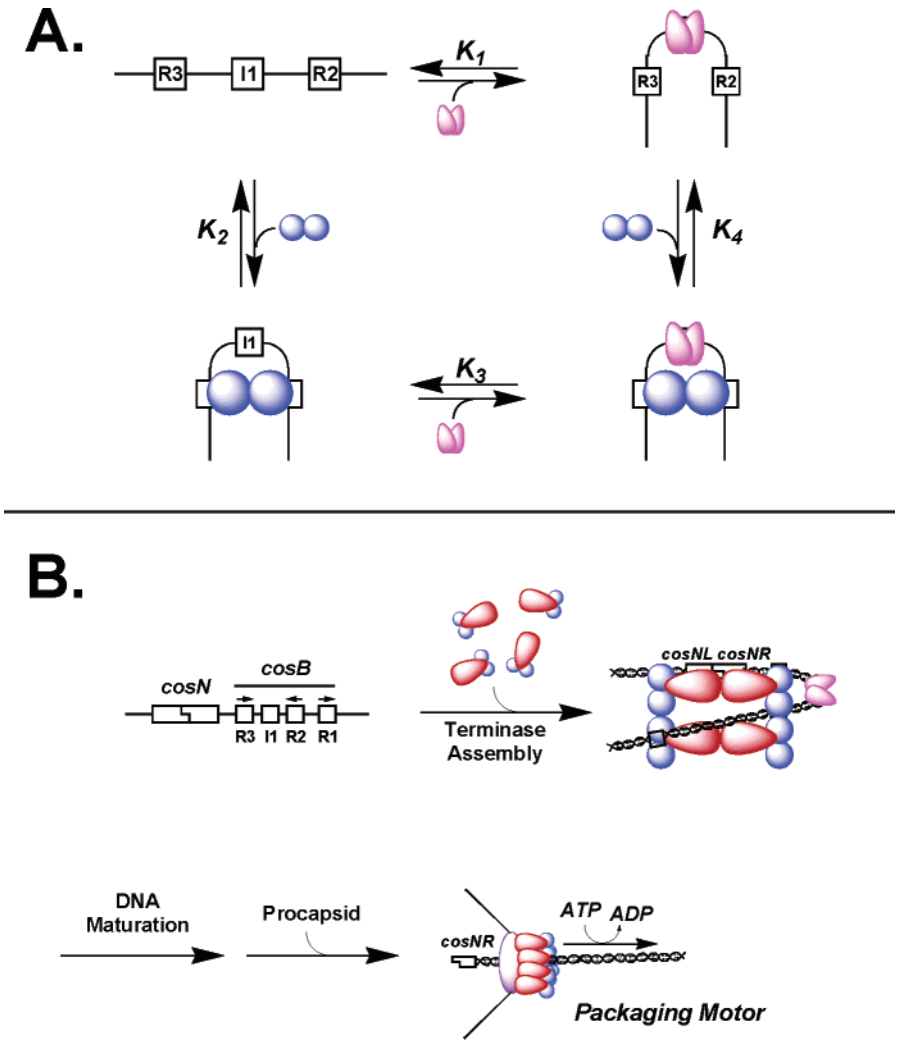

FIGURE 6: (A) Model for cooperative binding of IHF (purple lobes) and gpNu1 (blue spheres) to *cos*-DNA. Each protein binds to *cos*-DNA and introduces a bend in the duplex. Binding of the second protein is facilitated by "pre-bending" of the duplex. Thus, the dissociation constants $K_1 > K_3$ and $K_2 > K_4$. (B) Model for terminase assembly at the *cos*-site. The terminase protomer is a heterotrimer composed of one gpA subunit tightly associated with a gpNu1 dimer. Four protomers assemble at *cos* resulting in bending of the duplex into a "packasome" complex. Duplex bending by a gpNu1 dimer bound to the R3 and R2 elements is central to the assembly of the packaging machinery. DNA maturation includes duplex nicking and separation of the DNA strands. Details are presented in the text.

The second surprise was that gpNu1 binds to *cos*-DNA to yield a *single* gel-retarded complex at all intermediate protein concentrations in the binding experiment. The model shown in Figure 1C is consistent with this observation since it predicts that a single gpNu1 dimer binds to *cosB* and is expected to yield a single nucleoprotein complex, as observed. It is noteworthy that the proposed model also predicts that the data should be well-described by a simple Langmuir binding analysis. This is clearly not the case, however. Accurate fitting of the data requires that the Hill coefficient (n) "float" in the analysis, which yields a value of $n = 1.3-2$ depending on the substrate (see Tables 1−3). Of note, a similar Hill coefficient is observed when IHF binds to *cos* ($n \approx 1.7$; Tables 1 and 2). This phenomenon has been previously reported with IHF binding to the H′ sequence of the lambda genome (*45*). A Hill coefficient greater than unity is typically interpreted to indicate coupled protein dimerization and DNA binding events (*53*). The dissociation constant for both proteins remains unknown, and it is feasible that the gpNu1 homodimer and/or the IHF heterodimer dissociates into its composite monomers at the low concentrations used in this study. In this case, a Hill coefficient > 1 might indicate that protein dimerization is coupled to DNA binding. We disfavor this explanation, as thermally induced unfolding experiments suggest that folding and dimerization of gpNu1 is thermodynamically linked (Meyer and Catalano, unpublished results). Thus, any gpNu1 "monomer" that forms in solution is likely denatured and nonfunctional. Alternatively, these results may reflect cooperative binding to nonspecific DNA coupled to specific recognition of *cos* DNA sequences, as proposed for IHF binding to the H′ site (*45*). The latter is consistent with the relatively low concentration of salt used in these experiments (50 mM NaCl) and the weak discrimination of both proteins for their specific DNA sequences.

What is the Role of the R1 Element in gpNu1 Assembly at cosB? The model presented in Figure 1C is consistent with all of the available data, and we suggest that the proposed gpNu1−*cosB* interaction plays a pivotal role in site-specific assembly of the motor complex on viral DNA. The gpNu1 subunit also interacts with the R1 element of *cosB*; however, the nature and function of this interaction is less clear. Within this context, we note that biochemical and biophysical studies have defined a hydrophobic self-association domain of gpNu1 (residues 100−141). This region of the protein is

responsible for higher-order interactions of gpNu1 dimers and is also required for high-affinity DNA-binding interactions (*29*, *30*). This suggests that higher-order assemblies of the gpNu1 dimer may be required for efficient assembly at *cos*. It is tempting to speculate that a second gpNu1 dimer binds to the R1 element and to a "nonspecific" sequence within *cosB* to introduce additional bending into the duplex. This would yield a nucleoprotein complex where the DNA is bent and perhaps wrapped by the assembly proteins. Consistent with this hypothesis, DNase protection studies have shown that terminase holoenzyme covers roughly 200 bp of duplex DNA surrounding the *cos* site, and the authors suggested that "an organized protein−DNA complex involving several terminase protomers is involved" (*54*). Thus, we suggest that, while interactions of a gpNu1 dimer with the R3−R2 elements are essential, these may be supported by additional, higher-order interactions that include specific binding of a second gpNu1 dimer to the R1 element. We note that genetic studies have shown that the R1 element is dispensable to virus assembly in the presence of IHF (*55*). Further, our data indicate that deletion of the R1 element (in the minimal *cos2*-DNA substrate) does not affect gpNu1 binding affinity. In sum, the data suggest that that the gpNu1−R1 interaction introduces additional stability into the bent complex, a role that may be satisfied by IHF alone.

What is the Structure of the Packaging Motor? Studies on soluble deletion mutants of gpNu1 clearly establish that the DNA-binding domain forms a stable dimer structure under all conditions examined (*31*, *33*). It is thus likely that a gpNu1 dimer plays a functional role in DNA recognition and that the dimeric nature of gpNu1 is retained in the functional holoenzyme complex. Consistent with this hypothesis, biochemical and biophysical studies indicate that a gpNu1 dimer associates with one gpA subunit to form a stable heterotrimer (*56*). Furthermore, we have recently demonstrated that four of these heterotrimers assemble into a ring-like structure that possesses DNA maturation and DNA packaging activities (Maluf and Catalano, manuscript in preparation). We propose that the bona fide packaging motor complex is composed of a terminase ring structure assembled at the *cos* site. We further propose that the linchpin for this assembly is provided by interaction of a gpNu1 dimer with the R3−R2 elements of *cosB*, as shown in Figure 6B. Biophysical and structural studies currently underway in our laboratory seek to define the structure of terminase holoenzyme and the nucleoprotein packaging complexes.

DNA Bending in Biology. Data presented here clearly show that gpNu1 binds to *cos*-DNA and introduces a strong bend in the duplex. DNA bending is a common theme in biology and has been shown to play an important role in processes such as transcriptional regulation (*57*, *58*), integrative recombination (*59*), and condensation of genomic DNA (*60*). For instance, the cyclic AMP receptor protein (CPR) has been shown to bind multiple promoters in *E. coli* and induce a bend in the DNA structure (*43*). Formation of these bent structures results in either stimulation or repression of transcription, depending on the promoter. The bend in DNA thus acts as a form of regulation and is pivotal in assembly of transcriptional complexes. Similarly, the virally encoded Int and Xis proteins are involved in integration and excision, respectively, of the lambda genome into host DNA (*35*, *59*, *61*). It has been shown that these proteins, in conjunction with IHF, strongly bend duplex DNA to form an active synaptic complex (*59*). We suggest that bending of duplex DNA by terminase enzymes may represent a general mechanism for the recognition of viral DNA and the regulation of genome packaging in dsDNA viruses.

ACKNOWLEDGMENT

The authors thank Dr. Qin Yang for guidance with the initial EMS experiments and for helpful discussions. We further express our appreciation to Drs. Michael Feiss, Nasib Karl Maluf, and David Bain for helpful discussions and critical review of this manuscript.

REFERENCES

1. Casjens, S. R. (1985) An Introduction to Virus Structure and Assembly, in *Virus Structure and Assembly* (Casjens, S. R., Ed.) pp 1−28, Jones and Bartlett Publishers, Inc., Boston, MA.
2. Black, L. W. (1989) DNA Packaging in dsDNA Bacteriophages, *Annu. Rev. Microbiol. 43*, 267−292.
3. Catalano, C. E. (2005) Viral Genome Packaging Machines: An Overview, in *Viral Genome Packaging Machines: Genetics, Structure and Mechanism* (Catalano, C. E., Ed.) pp 1−4, Landes Bioscience/Eurekah.com, Georgetown, TX.
4. Murialdo, H. (1991) Bacteriophage Lambda DNA Maturation and Packaging, *Annu. Rev. Biochem. 60*, 125−153.
5. Fields, B. N., Knipe, D. M., and Howley, P. M. (1996) *Fields Virology*, 3rd ed., Lippincott-Raven Publishers, Philadelphia, PA.
6. Fujisawa, H., and Morita, M. (1997) Phage DNA Packaging, *Genes Cells 2*, 537−545.
7. Rubinchik, S., Parris, W., and Gold, M. (1994) The in Vitro ATPases of Bacteriophage Lambda Terminase and Its Large Subunit, Gene Product A, *J. Biol. Chem. 269*, 13586−13593.
8. Rubinchik, S., Parris, W., and Gold, M. (1994) The in Vitro Endonuclease Activity of Gene Product A, the Large Subunit of Bacteriophage Lambda Terminase, and Its Relationship to the Endonuclease Activity of the Holoenzyme, *J. Biol. Chem. 269*, 13575−13585.
9. Rubinchik, S., Parris, W., and Gold, M. (1995) The in Vitro Translocase Activity of Lambda Terminase and Its Subunits, *J. Biol. Chem. 270*, 20059−20066.
10. Parris, W., Rubinchik, S., Yang, Y.-C., and Gold, M. (1994) A New Procedure for the Purification of the Bacteriophage Lambda Terminase Enzyme and Its Subunits, *J. Biol. Chem. 269*, 13564−13574.
11. Woods, L., Terpening, C., and Catalano, C. E. (1997) Kinetic Analysis of the Endonuclease Activity of Phage Lambda Terminase: Assembly of a Catalytically-Competent Nicking Complex is Rate-Limiting, *Biochemistry 36*, 5777−5785.
12. Woods, L., and Catalano, C. E. (1999) Kinetic Characterization of the GTPase Activity of Phage Lambda Terminase: Evidence for Communication Between the Two "NTPase" Catalytic Sites of the Enzyme, *Biochemistry 38*, 14624−14630.
13. Feiss, M., and Catalano, C. E. (2005) Bacteriophage Lambda Terminase and the Mechanism of Viral DNA Packaging, in *Viral Genome Packaging Machines: Genetics, Structure and Mechanism* (Catalano, C. E., Ed.) pp 5−39, Landes Bioscience/Eurekah.com, Georgetown, TX.
14. Parris, W., Davidson, A., Keeler, C. L., and Gold, M. (1988) The *Nu1* Subunit of Bacteriophage Lambda Terminase, *J. Biol. Chem. 263*, 8413−8419.
15. Yang, Q., Hanagan, A., and Catalano, C. E. (1997) Assembly of a Nucleoprotein Complex Required for DNA Packaging by Bacteriophage Lambda, *Biochemistry 36*, 2744−2752.
16. Yang, Q., and Catalano, C. E. (2004) A Minimal Kinetic Mechanism for a Viral DNA Packaging Machine, *Biochemistry 43*, 289−299.
17. Bear, S., Court, D., and Friedman, D. (1984) An Accessory Role for *Escherichia coli* Integration Host Factor: Characterization of a Lambda Mutant Dependent Upon Integration Host Factor for DNA Packaging, *J. Virol. 52*, 966−972.
18. Shinder, G., and Gold, M. (1988) The Nu1 Subunit of Bacteriophage Lambda Terminase Binds to Specific Sites in *cos* DNA, *J. Virol. 62*, 387−392.

19. Feiss, M., Fogarty, S., and Christiansen, S. (1988) Bacteriophage Lambda DNA Packaging: A Mutant Terminase that is Independent of Integration Host Factor, *Mol. Gen. Genet. 212*, 142−148.
20. Mendelson, I., Gottesman, M., and Oppenheim, A. B. (1991) HU and Integration Host Factor Function as Auxiliary Proteins in Cleavage of Phage Lambda Cohesive Ends by Terminase, *J. Bacteriol. 173*, 1670−1676.
21. Xin, W., Cai, Z.-H., and Feiss, M. (1993) Function of IHF in λ DNA Packaging. II. Effects of Mutations Altering the IHF Binding Site and the Intrinsic Bend in *cosB* on Lambda Development, *J. Mol. Biol. 230*, 505−515.
22. Gold, M., and Parris, W. (1986) A Bacterial Protein Requirement for the Bacteriophage Lambda Terminase Reaction, *Nucleic Acids Res. 14*, 9797−9809.
23. Tomka, M. A., and Catalano, C. E. (1993) Physical and Kinetic Characterization of the DNA Packaging Enzyme from Bacteriophage Lambda, *J. Biol. Chem. 268*, 3056−3065.
24. Yang, Q., and Catalano, C. E. (2003) Biochemical Characterization of Bacteriophage Lambda Genome Packaging in Vitro, *Virology 305*, 276−287.
25. Gaussier, H., Yang, Q., and Catalano, C. E. (2005) Building a Virus from Scratch: Assembly of an Infectious Virus Using Purified Protein Components in a Rigorously Defined Biochemical Assay System, *J. Mol. Biol. 357*, 1154−1166.
26. Murialdo, H., Davidson, A., Chow, S., and Gold, M. (1987) The Control of Lambda DNA Synthesis, *Nucleic Acids Res. 15*, 119−140.
27. Meyer, J. D., Hanagan, A., Manning, M. C., and Catalano, C. E. (1998) The Phage Lambda Terminase Enzyme: 1. Reconstitution of the Holoenzyme from the Individual Subunits Enhances the Thermal Stability of the Small Subunit, *Int. J. Biol. Macromol. 23*, 27−36.
28. Hang, J. Q., Woods, L., Feiss, M., and Catalano, C. E. (1999) Cloning, Expression, and Biochemical Characterization of Hexa-Histidine-Tagged Terminase Proteins, *J. Biol. Chem. 274*, 15305−15314.
29. Yang, Q., de Beer, T., Woods, L., Meyer, J., Manning, M., Overduin, M., and Catalano, C. E. (1999) Cloning, Expression, and Characterization of a DNA Binding Domain of gpNu1, a Phage Lambda DNA Packaging Protein, *Biochemistry 38*, 465−477.
30. Yang, Q., Berton, N., Manning, M. C., and Catalano, C. E. (1999) Domain Structure of gpNu1, a Phage Lambda DNA Packaging Protein: Identification of Self-Association and gpA-Interactive Domains, *Biochemistry 38*, 14238−14247.
31. Bain, D. L., Berton, N., Ortega, M., Baran, J., Yang, Q., and Catalano, C. E. (2001) Biophysical Characterization of the DNA Binding Domain of gpNu1, a Viral DNA Packaging Protein, *J. Biol. Chem. 276*, 20175−20181.
32. de Beer, T., Meyer, J., Ortega, M., Yang, Q., Maes, L., Duffy, C., Berton, N., Sippy, J., Overduin, M., Feiss, M., and Catalano, C. E. (2002) Insights into Specific DNA Recognition During the Assembly of a Viral Genome Packaging Machine, *Mol. Cell 9*, 981−991.
33. Gaussier, H., Ortega, M. E., Maluf, N. K., and Catalano, C. E. (2005) Nucleotides Regulate the Conformational State of the Small Terminase Subunit from Bacteriophage Lambda: Implications for the Assembly of a Viral Genome-Packaging Motor, *Biochemistry, 44*, 9645−9656.
34. Jordan, S. R., and Pabo, C. O. (1988) Structure of the Lambda Complex at 2.5 Å Resolution: Details of the Repressor-Operator Interactions, *Science 242*, 893−899.
35. Moitoso de Vargas, L., Kim, S., and Landy, A. (1989) DNA Looping Generating by DNA Bending Protein IHF and the Two Domains of Lambda Integrase, *Science 244*, 1457−1461.
36. Kosturko, L. D., Daub, E., and Murialdo, H. (1989) The Interaction of *E. coli* Integration Host Factor and Lambda *cos* DNA: Multiple Complex Formation and Protein-Induced Bending, *Nucleic Acids Res. 17*, 317−333.
37. Rice, P. A., Yang, S.-W., and Mizuuchi, K. (1996) Crystal Structure of an IHF-DNA Complex: A Protein-Induced DNA U-Turn, *Cell 87*, 1295−1306.
38. Nash, H. A. (1996) The HU and IHF Proteins: Accessory Factors for Complex Protein-DNA Assemblies, in *Regulation of Gene Expression in E. coli* (Lin, E. C. C., and Lynch, A. S., Eds.) pp 149−179, R. G. Landes Co., Austin, TX.
39. Hanagan, A., Meyer, J. D., Johnson, L., Manning, M. C., and Catalano, C. E. (1998) The Phage Lambda Terminase Enzyme: 2. Refolding of the gpNu1 Subunit from the Detergent-Denatured and Guanidinium Hydrochloride-Denatured State Yields Different Oligomerization States and Altered Protein Stabilities, *Int. J. Biol. Macromol. 23*, 37−48.
40. Nash, H. A., Robertson, C. A., Flamm, E., Weisberg, R. A., and Miller, H. I. (1987) Overproduction of *Escherichia coli* Integration Host Factor, a Protein with Nonidentical Subunits, *J. Bacteriol. 169*, 4124−4127.
41. Maniatis, T., Firtsch, E. F., and Sambrook, J. (1982) *Molecular Cloning, A Laboratory Manual*, 2nd ed., Cold Spring Harbor Laboratory Press, Cold Spring Harbor Laboratory, New York.
42. Carey, J. (1991) Gel Retardation, *Methods Enzymol. 208*, 103−118.
43. Kim, J., Zwieb, C., Wu, C., and Adhya, S. (1989) Bending of DNA by Gene-Regulatory Proteins: Construction and Use of a DNA Bending Vector, *Gene 85*, 15−23.
44. Thompson, J. F., and Landy, A. (1998) Empirical Estimation of Protein-Induced DNA Bending Angles: Applications to Lambda Site-Specific Recombination Complexes, *Nucleic Acids Res. 16*, 9687−9705.
45. Dhavan, G. M., Crothers, D. M., Chance, M. R., and Brenowitz, M. (2002) Concerted Binding and Bending of DNA by *Eschericia coli* Integration Host Factor, *J. Mol. Biol. 315*, 1027−1037.
46. Nash, H. A., and Robertson, C. A. (1981) Purification and Properties of the *Escherichia coli* Protein Factor Required for λ Integrative Recombination, *J. Biol. Chem. 256*, 9246−9253.
47. Granston, A. E., Alessi, D. M., Eades, L. J., and Friedman, D. I. (1988) A Point Mutation in the *Nu1* Gene of Bacteriophage Lambda Facilitates Growth in *E. coli* with *himA* and *gyrB* Mutations, *Mol. Gen. Genet. 212*, 149−156.
48. Catalano, C. E., Cue, D., and Feiss, M. (1995) Virus DNA Packaging: The Strategy Used by Phage Lambda, *Mol. Microbiol. 16*, 1075−1086.
49. Darling, P. J., Holt, J. M., and Akers, G. K. (2000) Coupled Energetics of λ *cro* Repressor Self-Assembly and Site-Specific DNA Operator Binding I: Analysis of *cro* Dimerization from Nanomolar to Micromolar Concentrations, *Biochemistry 39*, 11500−11507.
50. Chadwick, P., Pirrotta, V., Steinberg, N., Hopkins, N., and Ptashne, M. (1971) The λ and Phage 434 Repressors, *Cold Spring Harbor Symp. Quant. Biol. 35*, 283−294.
51. Aggarwal, A. K., Rodgers, D. W., Drottar, M., Ptashne, M., and Harrison, S. C. (1988) Recognition of a DNA Operator by the Repressor of Phage 434: A View at High Resolution, *Science 242*, 899−907.
52. Yeo, A., Kosturko, L. D., and Feiss, M. (1990) Structure of the Bacteriophage Lambda Cohesive End Site: Bent DNA on Both Sides of the Site, *cosN*, at which Terminase Introduces Nicks during Chromosome Maturation, *Virology 174*, 329−334.
53. Wong, I., and Lohman, T. (1995) Linkage of Protein Assembly to Protein-DNA Binding, *Methods Enzymol. 259*, 95−127.
54. Higgins, R. R., and Becker, A. (1995) Interaction of Terminase, the DNA Packaging Enzyme of Phage Lambda, with Its *cos* Substrate, *J. Mol. Biol. 252*, 31−46.
55. Cue, D., and Feiss, M. (1992) Genetic Analysis of *cosB*, the Binding Site for Terminase, the DNA Packaging Enzyme of Bacteriophage Lambda, *J. Mol. Biol. 228*, 58−71.
56. Maluf, N. K., Yang, Q., and Catalano, C. E. (2005) Self-Association Properties of Bacteriophage Lambda Terminase Holoenzyme: Implications for the DNA Packaging Motor, *J. Mol. Biol. 347*, 523−542.
57. Adhya, S. (1989) Multipartite Genetic Control Elements: Communication by DNA Loop, *Annu. Rev. Genet. 23*, 227−250.
58. Rees, W. A., Keller, R. W., Vesenka, J. P., Yang, G., and Bustamante, C. (1993) Evidence of DNA Bending in Transcription Complexes Imaged by Scanning Force Microscopy, *Science 260*, 1646−1649.
59. Landy, A. (1989) Dynamic, Structural, and Regulatory Aspects of Lambda Site-Specific Recombination, *Annu. Rev. Biochem. 58*, 913−949.
60. Wu, H.-M., and Crothers, D. M. (1984) The Locus of Sequence-Directed and Protein-Induced DNA Bending, *Nature 308*, 509−513.
61. Kim, S., and Landy, A. (1992) Lambda Int Protein Bridges Between Higher Order Complexes at Two Distant Chromosomal Loci *att*L and *att*R, *Science 256*, 198−203.

BI052284B